Available online at www.sciencedirect.com
ScienceDirect
Energy Procedia 54 (2014) 718 – 724
Energy Procedia

4th International Conference on Advances in Energy Research 2013, ICAER 2013

Carbon Coated Submicron sized-$LiFePO_4$: Improved High Rate Performance Lithium Battery Cathode

S. Sarkar[a], S. Mitra[a,*]

[a] *Electrochemical Energy Lab, Dept. of Energy Science & Engineering, Indian Institute of Technology Bombay, Mumbai-76, India*

Abstract

High rate performance along with high specific energy is the foremost criteria for advanced lithium-ion batteries. To improve the high rate capability and cyclic performance of $LiFePO_4$, continuous carbon coating technique was adopted. The carbon coated submicron-$LiFePO_4$ (C-$LiFePO_4$), composite was successfully prepared via. a solution based method followed by carbonization process. C-$LiFePO_4$ composite exhibits excellent electrochemical properties, including superior high rate cyclic performance and cyclic stability at relatively high charge-discharge current rate at 20°C. *In-situ* continuous carbon coating exercises a significant impact on the electronic conduction and the unique composite demonstrates excellent electrochemical performance with reversible capacity of 148 mAh g^{-1} and 114 mAh g^{-1} at 1C and 10C current rate respectively.

Selection and peer-review under responsibility of Organizing Committee of ICAER 2013

Keywords: High power density cathode, $LiFePO_4$ composite, Lithium-ion batteries, Co-precipitation method

1. Introduction

$LiFePO_4$ based lithium-ion battery is one of the most advanced technology in recent times for electric vehicles, plug-in hybrid vehicles and other high-rate applications such as renewable energy storage and power tools [1-3]. This is possible due to the many unique features of this compound which include reasonable high capacity (~ 170 mAh g^{-1}), two phase electrochemical process which evolves with a flat plateau at 3.5 V *vs.* Li/Li^+, attractive cost as compared to $LiCoO_2$ and most significantly, safer than other cathode materials in high charge-discharge situations [4]. Despite these unique features, it suffers from poor electrical conductivity ($\sigma = 10^{-9}/10^{-10}$ Scm^{-1}) [5], ionic

* Corresponding author. Tel.: (+91-22) 2576 4897/7849,
E-mail address: sagar.mitra@iitb.ac.in

Selection and peer-review under responsibility of Organizing Committee of ICAER 2013
doi:10.1016/j.egypro.2014.07.312

conductivity (10^{-10} to 10^{-9} Scm^{-1}) [5-6] and ionic diffusivity (10^{-17} to 10^{-12} cm^2s^{-1}) [7] thereby resulting in poor electrochemical performance. In order to enhance the electronic conductivity, several groups have oriented their research in the same area. In the literature, two types of approaches have been reported to address the specific problems. First, is the reduction of particle size [5, 8, 9] which consequently reduces the lithium-ion diffusion path length and second is the preparation of composites with continuous conductive coating, such as carbon [10], graphene [11], metal doping [12], metal oxide coating [13] and surface modifications by nano-sized metals like Cu [14-15] and Ag [15]. In recent research, nano-$LiFePO_4$ particles have been used to exhibit ultrafast battery performance [8]. However, the practical battery performance with $LiFePO_4$ nano-particles remains challenging and divisive due to poor understanding of lithium intercalation mechanism at high rates. Highly anisotropic transport of Li-ions [16-17], size-dependent diffusivity [18] and its strong affinity to separate into Li-rich and Li-poor phases at nanoscale hinders their electrochemical performance at high rates [19-21]. It has also been observed that there is a variation in the reported values of the diffusivity and exchange current density for nano-sized $LiFePO_4$ material by few orders of magnitude [18, 22-26]; illustrates the fundamental ambiguity in the reaction kinetics of nano-particles which regulate battery performance. However, we could easily avoid such fundamental issues of nano-sized $LiFePO_4$ particles by using relatively larger size (~ 200 nm) particles. For example, C. Delacourt *et al.* have shown that carbon free $LiFePO_4$ having particle size around 140 nm can deliver capacity of 147 $mAhg^{-1}$ at 5 C-rate [27]. Similarly, Y. Ding *et al.* have also shown capacity 120 mAh g^{-1} at 5 C-rate with $LiFePO_4$ / graphene composites with 100 nm average particle size [28]. In this respect, few different material preparation methods have been reported in the literature along with improved electrochemical activity [29-31]. Based on the recent literature, it is believed that the electrochemical performance of $LiFePO_4$ electrode can be improved by constructing the facile pathway for electron transport and ion diffusion through the active materials [5, 32, 33].

Continuous carbon coating to the larger pristine $LiFePO_4$ particle technique has been selected for the current study. Along with the previous approaches of making $LiFePO_4$ composites [31, 34-35], we have created a continuous layer of carbon on the surface of submicrometer sized $LiFePO_4$ which shows excellent electrochemical performance at high rates. The C-$LiFePO_4$ composite was prepared by simple co-precipitation technique. The sub-micrometer sized $LiFePO_4$ composite with continuous carbon coating overcomes the poor electronic conductivity, Lithium-ion diffusion limitation and provides excellent electrochemical performance at high rates. The observed high rate electrochemical performance of continuous carbon layer on sub-micrometer sized $LiFePO_4$ particles is a unique feature of this report.

2. Experimental Section

Carbon coated submicron sized $LiFePO_4$ (C-$LiFePO_4$) samples were prepared by co-precipitation technique followed by sucrose assisted carbonization. At first, separate aqueous solution of Li(OH) (99%, SRL, India), $FeSO_4.7H_2O$ (98 %, Fisher Sc., India) and $(NH_4)_2HPO_4$ (99 %, Merck, India) were prepared in the molar ratio of 3:1:1 (Li:Fe:P). Later on, Li(OH) solution was added drop wise in the $(NH_4)_2HPO_4$ solution under vigorous stirring, thus forming Li_3PO_4. Further, $FeSO_4.7H_2O$ solution was added drop wise in the above solution to form green color precipitate. The precipitate was washed several times using de-ionized water and then dried at 60°C. Then the dried sample was mixed with solid sucrose (Merck, India) and ball-milled for 10 hours at 250 rpm. The ball-milled sample was then annealed at 600°C in 5% H_2 + 95% N_2 atmosphere for 6 hours and the color of the sample changed to black due to formation of carbon.

The phase analysis was carried out by Philips X'pert X-ray diffractometer with a Cu-K_α radiation. The microstructure and morphology of sample were determined by field emission gun scanning electron microscope (FEG-SEM, JSM-7600F) and high resolution field emission transmission electron microscope (HR-TEM, Jeol-2100F). Carbon content was quantified by Carbon Hydrogen Nitrogen analysis (CHN, Flash EA 1112 series, Thermo Finnigan).

Electrochemical performance of the material was carried out on Swagelok type cell. The complete cell comprises of a cathode (C-$LiFePO_4$), glass microfiber filter (Whatman, 47 mm ø) as a separator soaked in electrolyte (LP-30,

Merck, Germany) and lithium foil as counter electrode respectively. The electrode material (75 wt%) was hand grinded with of 20% of carbon black (Super C-65, Timcal) and 5% of PVDF (Sigma Aldrich) for half an hour. The slurry of mixed powder was prepared by adding NMP (Qualigens, India) as solvent. Slurry was then cast on aluminum foil with the help of doctor blade. After casting, the electrode foil was dried in vacuum oven for 12 hours at 60^{o}C. The electrode film was then cut in the form of circular disk of different diameters like 10 mm and 12 mm, respectively. The electrochemical charge-discharge was performed in Bio-logic VMP-3 and Arbin BT2000 with various current rates at 20±2 °C.

3. Results and Discussion

Fig. 1a shows, X-ray diffraction (XRD) pattern of the C-$LiFePO_4$ which illustrates well defined crystallites and phase pure $LiFePO_4$ compound. All the diffraction peaks of C-$LiFePO_4$ sample were indexed with an orthorhombic structure (*Pnma*), confirming to the JCPDS Card No. 83-2092. The broader background around 20-30 (2θ value) in XRD, suggests the presence of amorphous carbon of C-$LiFePO_4$ composite sample. Lattice parameters for the C-$LiFePO_4$ were measured to be a=10.30Å, b=6.05Å, c=4.67Å, with unit cell volume of 291.34 $Å^3$ which is close to reported value in JCPDS Card No. 83-2092. The amount of carbon in the composite was quantified by CHN analysis and amount found to be ~8.1 %.

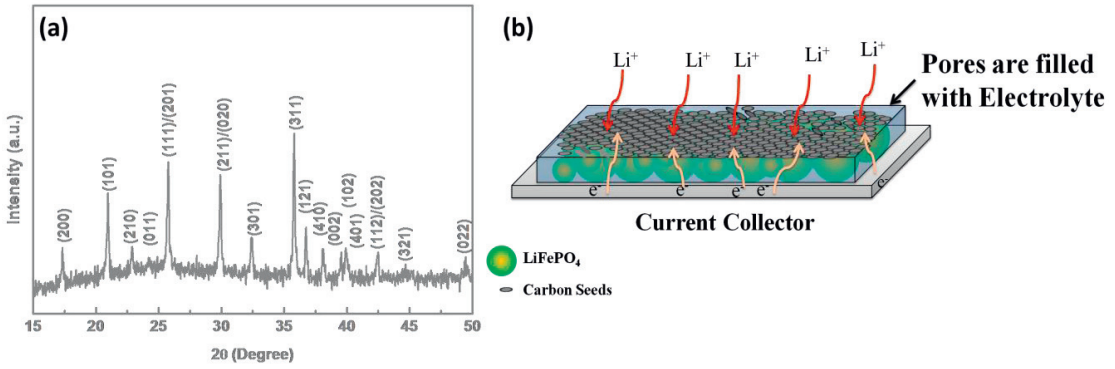

Fig.1. a) XRD pattern of C-$LiFePO_4$ composite, and b) Schematic of continuous carbon seeds on the surface of $LiFePO_4$ particles.

Schematic illustration of submicron sized C-$LiFePO_4$ composite is shown in fig. 1b, which describes the concept of well connected carbon seeds spread on the surface of submicron-sized $LiFePO_4$, which helps in fast diffusion of the lithium-ions and electrons to enhance the electrochemical performance. The surface morphology and crystal arrangement of the C-$LiFePO_4$ composite powder was investigated by FEG-SEM and HR-TEM. Fig. 2a shows the FEG-SEM image of C-$LiFePO_4$, the image illustrates the formation of carbon seeds on the surface of $LiFePO_4$ particle which is well distributed and connected with in the $LiFePO_4$ particles which are also confirmed by HR-TEM analysis, shown in fig. 2b. As shown in fig. 2b, the carbon particles are well connected with each of the $LiFePO_4$ particles (black dotted line) and can provide better electronic bridge between active materials. From Fig. 2a and 2b, it is evident that the particle size of $LiFePO_4$ in the order of ~ 150-250 nm with occasional existence of ~ 100 nm size particles. Fig. 2c and 2d shows lattice patterning and selected area electron diffraction (SAED) of C-$LiFePO_4$ particle; which shows pure crystalline phase of $LiFePO_4$. The typical lattice fringes width of the order of 3.4 Å and 3.9 Å are observed, which are consistent with the (201) and (210) planes of orthorhombic phase (space group: *Pnma*) of $LiFePO_4$.

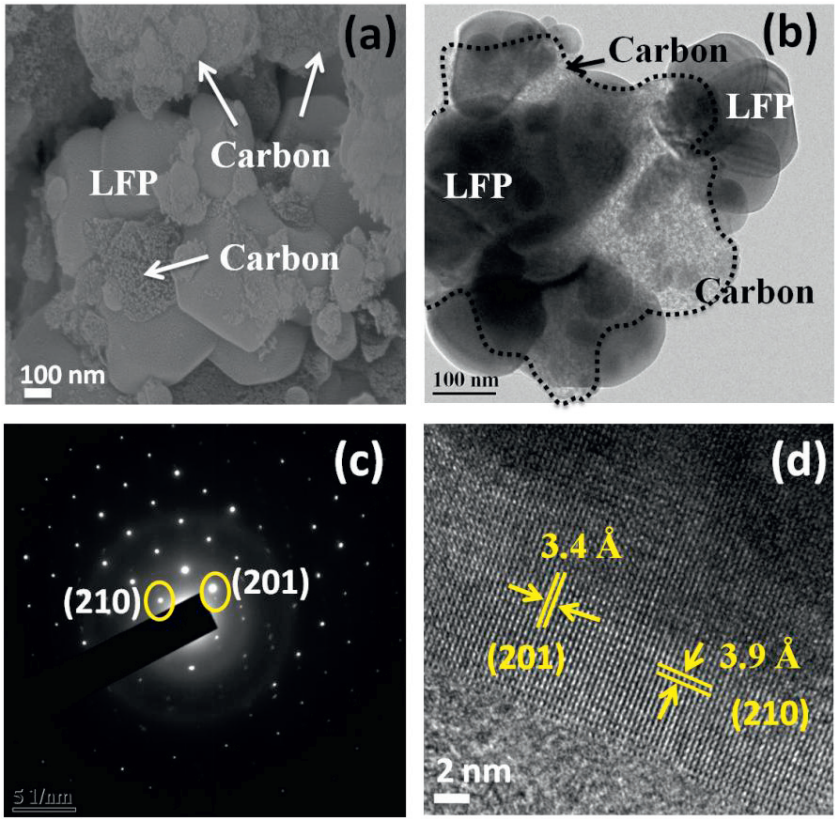

Fig. 2. (a) FEG-SEM of C-$LiFePO_4$, (b) HR-TEM micrograph of C-$LiFePO_4$, (c) SAED pattern of C-$LiFePO_4$ and (d) Lattice fringes of C-$LiFePO_4$ particle.

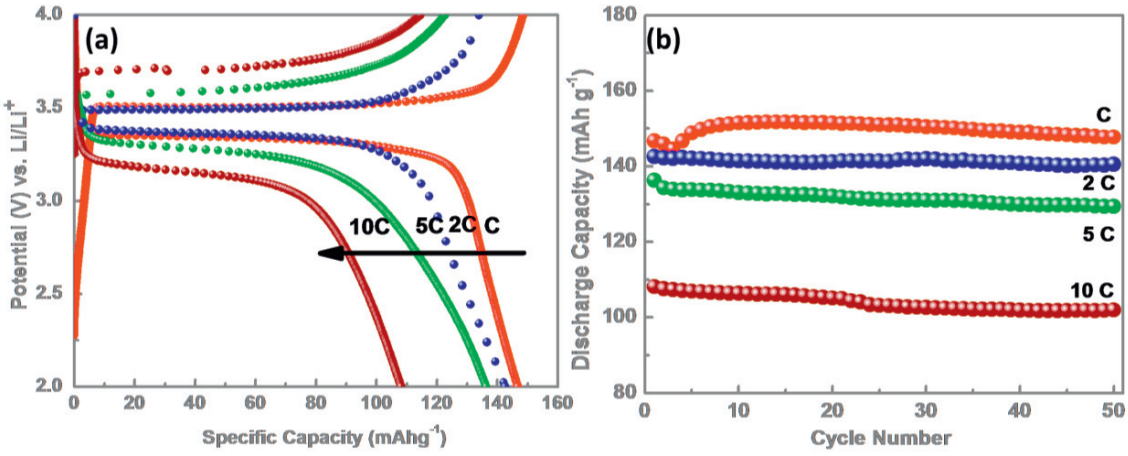

Fig. 3. (a) First cycle of Charge-Discharge characteristics of C-$LiFePO_4$ at various rates and (b) Discharge capacity *vs.* cycle number at various rates at 20°C.

Galvanostatic charge-discharge test for C-$LiFePO_4$ composite *vs.* Li/Li^+ was performed between 2.0 V-4.0 V *vs.* Li/Li^+ at various C-rates at 20°C. First charge/discharge of C-$LiFePO_4$ is shown in fig. 3a. As seen in the fig. 3a, C-$LiFePO_4$ redox couple shows plateau at ~3.44 V/3.3 V at 1 C and 2 C rates for intercalation/deintercalation process respectively. However, large polarization behaviour was observed at high current charge-discharge process (like 2 C to 10 C rate) which could be ascribed to the increase in ohmic drop due to electrolyte degradation and increase in charge transfer resistance, same as earlier reports [11, 36]. It is noteworthy that discharge profile of C-$LiFePO_4$ particles has shown larger plateau region and steep fall whereas in the case of nano-sized particles discharge profile showed short plateau with larger slope region (below 3V) as per earlier literature [37]. This trend is considered as capacitive (pseudo-capacitive effect) behaviour at the reaction interface [38] which has been reported for nano materials having high surface area [39-41]. So, it is beneficial to have submicron sized $LiFePO_4$ particles which contribute maximum capacity from the plateaus region as compared to the nano sized $LiFePO_4$. Further, in this case plateau region in the discharge profile of C-$LiFePO_4$ particles contributes 86.5 % of the total capacity at 1C-rate; which is quite satisfactory for high rate battery applications. The first discharge capacity of C-$LiFePO_4$ at different current rates are found to be 148 $mAhg^{-1}$, 142 $mAhg^{-1}$, 136 $mAhg^{-1}$ and 114 $mAhg^{-1}$ at 1C, 2C, 5C and 10 C-rate respectively as illustrated in fig. 3a which is compatible with recent results by Y. Wang *et al.* [30] using similar process. The excellent electrochemical performance is attributed to the formation of well distributed carbon particle around $LiFePO_4$ making very well electronic interconnects as shown in fig. 2a and 2b. The discharge capacity of C-$LiFePO_4$ *vs.* cycle number is shown in the fig. 3b for various C-rates. The capacity retention of C-$LiFePO_4$ is excellent throughout 50 cycles. The incredible improvement in rate capability and excellent cyclibility can be attributed to the favourable lithium-ion transport and three-dimensional electron transport. Above results indicate that the continuous carbon networks provide fast electronic transport during high rate charge-discharge processes, which is beneficial for C-$LiFePO_4$composite to exhibit excellent electrochemical performance at high current rates.

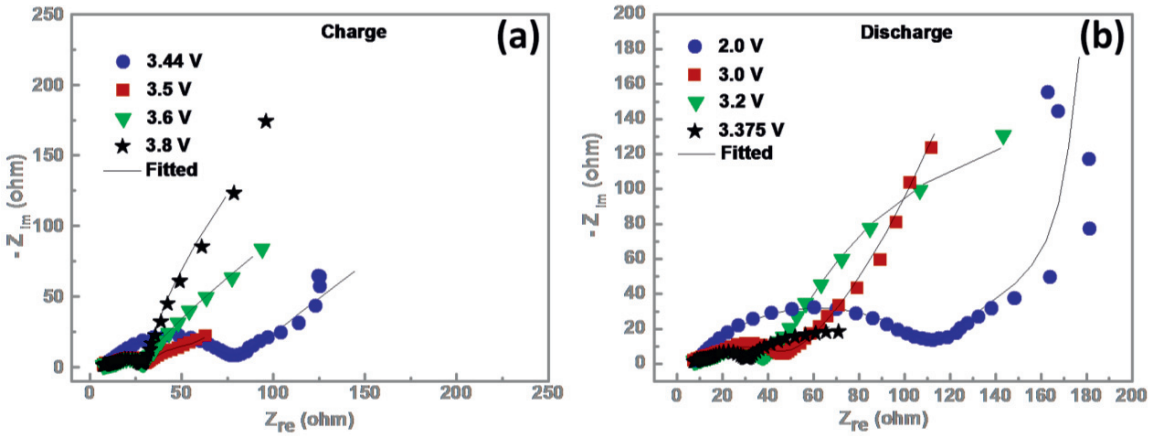

Fig. 4. Nyquist plot of C-$LiFePO_4$ at various (a) charge and (b) discharge process.

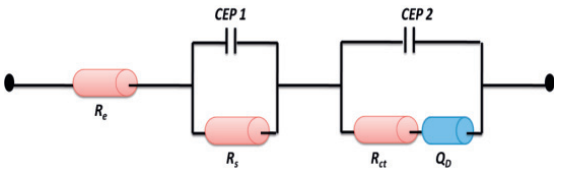

Fig. 5. Equivalent circuit model for Li/Electrolyte/C-$LiFePO_4$ half-cell.

To understand electrode kinetics of C-$LiFePO_4$, electrochemical impedance spectroscopy (EIS) experiments during 1st charge-discharge cycle was performed (fig. 4a and fig.4b). Lithium insertion reaction can be broadly classified as 1) electron transfer from current collector to active materials, 2) lithium-ion diffusion in solid-state matrix, 3) charge transfer from solid matrix to electrolyte solution and 4) lithium-ion diffusion in ionic media (electrolyte) with bulk lithium diffusivity [42]. The corresponding equivalent circuit for the two parallel RC circuit is represented in fig. 5, where R_e, R_s indicates the solution resistance, and resistance of lithium-ion migration process, respectively, whereas CPE 1 and CPE 2 represents as capacitance of the surface-passivating layer and double-layer capacitance, respectively. Similarly, R_{ct} was designate as charge transfer resistance and Z_W represents Warburg impedance. The excellent correlation between the experimental EIS experimental data and simulated curves indicates the accuracy of the model within the experimental error limits. It is quite distinct from the fig. 4 that the charge transfer resistances of C-$LiFePO_4$ decrease with decrease in the lithium content during charge process whereas reverse phenomenon is observed during discharge process, similar observation is established in LiV_3O_8 cathode [42, 43]. Therefore we can conclude that the material is transforming from an insulator to conductor when *x* decreases (charge process), while reverse is expected as observed form discharge process.

4. Conclusion

In this report, we have introduced a simple solution based technique to prepare submicron sized C-$LiFePO_4$ composite followed by sucrose assisted carbonization process. Submicron sized particles compared to nano-sized particles can alleviate extra surface reactions below 3 V region in the discharge profile so that the maximum capacity can be extracted from the plateau region. In this case, the side reactions below 3 V were minimal even at high rates of discharge process due to submicron sized $LiFePO_4$ particles. The high rate performance is attributed to the concept of having continuous carbon coating throughout the submicron sized $LiFePO_4$ particles. The C-$LiFePO_4$ electrode exhibited good discharge capacity of about 148 mAh g^{-1}, 142 mAh g^{-1}, 136 mAh g^{-1}, and 114 mAh g^{-1} at C, 2C, 5C and 10 C-rates respectively. The discharge capacity reported here at high rates is excellent and need attention. The capacity retention of C-$LiFePO_4$ composite was outstanding throughout 50 cycles at 20°C at various C-rates.

Acknowledgements

The authors are indebted to SAIF, IITB for their assistance with CHN, HR-TEM and FEG-SEM analysis.

References

[1] Tarascon, J-M, Armand, M. Issues and challenges facing rechargeable lithium batteries. Nature 2001: **414**: 359-367.
[2] Bruce P G, Scrosati B, Tarascon J-M. Nanomaterials for rechargeable lithium batteries. Angew. Chem. Int. Ed. 2008: **47:** 2930-2046.
[3] Wang Y, He P, Zhou H. Olivine $LiFePO_4$: development and future, Energy Environ. Sci 2011: **4**: 805-817.
[4] Padhi A K, Nanjundaswamy K S, Goodenough J B. Phospho-olivines as positive-electrode materials for rechargeable lithium batteries. J. Electrochem.Soc. 1997: **144**: 1188-1194.
[5] Gaberscek M, Dominko R, Jamnik J. Is small particle size more important than carbon coating? An example study on $LiFePO_4$ cathodes. Electrochem. Commun. 2007: **9**: 2778-2783.
[6] Wang C W, Sastry A M, Striebel K A, Zaghib K. Extraction of layerwise conductivities in carbon-enhanced, multilayered $LiFePO_4$ cathodes. J. Electrochem. Soc. 2005: **152**: A1001-1010.
[7] Prosini P P, Lisi M., Zane D, Pasquali M. Determination of the chemical diffusion coefficient of lithium in $LiFePO_4$. Solid State Ionics. 2002: **148**: 45-51.
[8] Kang B, Ceder G. Battery materials for ultrafast charging and discharging. Nature. 2009: **458**: 190-193.
[9] Herle P S, Ellis B, Coombs N, Nazar L F. Nano-network electronic conduction in iron and nickel olivine phosphates. Nat. Mater. 2004:**3**: 147-152.
[10] Ravet N, Goodenough, J B, Besner S, Simoneau M, Hovington P, Armand M. Improved iron based cathode material. Electrochem. Soc. Meeting Abstr. 1999: **196**: 127.
[11] Tang Y, Huang F, Bi H, Liu Z, Wan D. Highly conductive three-dimensional graphene for enhancing the rate performance of $LiFePO_4$ cathode. J. Power Sources. 2012: **203**: 130-134.
[12] Chung S Y, Bloking J T, Chiang Y M. Electronically conductive phospho-olivines as lithium storage electrodes. Nat. Mater. 2002: **1**: 123-128.

[13] Hu Y S, Guo Y G, Dominko R, Gaberscek M, Jamnik J, Maier J. Improved electrode performance of porous $LiFePO_4$ using RuO_2 as an oxidic nanoscale interconnect. Adv. Mater. 2007: **19**: 1963-1966.
[14] Croce F, Epifanio, A D, Hassoun J, Deptula A, Olezac T, Scrosati B. A novel concept for the synthesis of an improved $LiFePO_4$ lithium battery cathode. Electrochem. Solid-State Lett. 2002: **5**: A47-A50.
[15] Park K S, Son J T, Chung H T, Kim S J, Lee C H, Kang K T, Kim H G. Surface modification by silver coating for improving electrochemical properties of $LiFePO_4$. Solid State Communications. 2004: **129**: 311-314.
[16] Morgan D, Van der Ven A, Ceder G. Li conductivity in Li_xMPO_4 (M = Mn , Fe , Co , Ni) olivine materials. Electrochem. Solid-State Lett. 2004: **7**: A30-A32.
[17] Islam M S, Driscoll D J, Fisher C A J, Slater P R. Atomic-scale investigation of defects, dopants and lithium transport in the $LiFePO_4$ olivine-type battery material. Chem. Mater. 2005: **17**: 5085-5092.
[18] Malik R, Burch D, Bazant M, Ceder G, Particle size dependence of the ionic diffusivity. Nano Lett. 2010: **10**: 4123-4127.
[19] Chen G, Song X, Richardson T J. Electron microscopy study of the $LiFePO_4$ to $FePO_4$ phase transition, Electrochem. Solid-State Lett. 2006: **9**: A295-A298.
[20] Laffont, L., Delacourt, C., Gibot, P., Wu, M. Y., Kooyman, P., Masquelier, C., Tarascon, J. M. (2006) Study of the $LiFePO_4/FePO_4$ Two-Phase System by High-Resolution Electron Energy Loss Spectroscopy, Chem. Mater., **18**, 5520-5529.
[21] Ramana C V, Mauger A, Gendron F, Julien C M, Zaghib K. Study of the Li-insertion/extraction process in $LiFePO_4/FePO_4$. J. Power Sources. 2009: **187**: 555-564.
[22] Srinivasan V, Newman J. Discharge model for the lithium iron-phosphate electrode. J. Electrochem. Soc. 2004: **151**: A1517-A1529.
[23] Wang C S, Kasavajjula U S, Arce P E. A discharge model for phase transformation electrodes: formulation, experimental validation, and analysis. J. Phys. Chem. C. 2007: **111**: 16656-16663.
[24] Pasquali M, Dell'Era A, Prosini P P. Fitting of the voltage-Li^+ insertion curve of $LiFePO_4$. J. Solid State Electrochem. 2009: **13**: 1859-1865.
[25] Shenouda A Y, Liu H. K. Studies on electrochemical behaviour of zinc-doped $LiFePO_4$ for lithium battery positive electrode. J. Alloys Compd. 2009: **477**: 498-503.
[26] Zhu Y J, Wang C S. Galvanostatic intermittent titration technique for phase-transformation electrodes. J. Phys. Chem. C. 2010: **114**: 2830-2841.
[27] Delacourt C, Poizot P, Levasseur S, Masquelier C. Size effects on carbon-free $LiFePO_4$ powders. Electrochem. Solid-State Lett. 2006: **9**: A352-A355.
[28] Ding Y, Jiang Y, Xua F, Yin J, Ren H, Zhuo Q, Long Z, Zhang P. Preparation of nano-structured $LiFePO_4$/graphene composites by co-precipitation method. Electrochem. Commun. 2010:**12**: 10-13.
[29] Qin X, Wang X, Xiang H, Xie J, Li J, Zhou Y. Mechanism for hydrothermal synthesis of $LiFePO_4$ platelets as cathode material for lithium-ion batteries. J. Phys. Chem. C. 2010:**114**: 16806-16812.
[30] Wang Y, Sun B, Park J, Kim W S, Kim H S, Wang G. Morphology control and electrochemical properties of nanosize $LiFePO_4$ cathode material synthesized by co-precipitation combined with in situ polymerization. J. Alloys and Compounds. 2011: **509**: 1040-1044.
[31] Yang K, Deng Z, Suo J. Synthesis and characterization of $LiFePO_4$ and $LiFePO_4$/C cathode material from lithium carboxylic acid and Fe^{3+}. J. Power Sources. 2012: **201**: 274-279.
[32] Liu Y, Li X., Guo H, Wang Z, Peng W, Yang Y, Liang R. Effect of carbon nanotube on the electrochemical performance of C-$LiFePO_4$/graphite battery. J. Power Sources, 2008:**184**: 522-526.
[33] Patey T J, Hintennach A, Mantia F L, Novák P. Electrode engineering of nanoparticles for lithium-ion batteries-role of dispersion technique. J. Power Sources. 2009:**189**: 590-593.
[34] Zhao J, He J, Zhou J, Guo Y, Wang T, Wu S, Ding X, Huang R, Xue H. Facile synthesis for $LiFePO_4$ nanospheres in tridimensional porous carbon framework for lithium ion batteries. J. Phys. Chem. C. 2011: **115**: 2888-2894.
[35] Brochu F, Guerfi A, Trottier J, Kopeć M, Mauger A, Groult H, Julien C M, Zaghib K. Structure and electrochemistry of scaling nano C-$LiFePO_4$ synthesized by hydrothermal route: complexing agent effect. J. Power Sources. 2012: **214:** 1-6.
[36] Su C, Lu G, Xu L, Zhang C. Preparation of $LiFePO_4$/Carbon/PANI-CSA composite and its properties as high-capacity cathodes for lithium ion batteries. J. Electrochem. Soc. 2012: **159**: A305-A309.
[37] Yang H, Wu X L, Cao M H, Guo Y G. Solvothermal synthesis of $LiFePO_4$ hierarchically dumbbell-like microstructures by nanoplate self-assembly and their application as a cathode material in lithium-ion batteries. J. Phys. Chem. C. 2009: **113**: 3345-3351.
[38] Maier J. Nanoionics: ion transport and electrochemical storage in confined systems. Nat. Mater. 2005:**4**: 805-815.
[39] Wang J, Polleux J, Lim J, Dunn B. Pseudocapacitive contributions to electrochemical energy storage in TiO_2 (anatase) nanoparticles. J. Phys. Chem. C. 2007: **111**: 14925-14931.
[40] Zhang H, Li G R, An L P, Yan T Y, Gao X P, Zhu H Y. Electrochemical lithium storage of titanate and titania nanotubes and nanorods. J. Phys. Chem. C. 2007:**111**: 6143-6148.
[41] Luo J Y, Wang Y G, Xiong H M, Xia Y Y. Ordered mesoporous spinel $LiMn_2O_4$ by a soft-chemical process as a cathode material for lithium-ion batteries. Chem. Mater. 2007:**19**: 4791-4795.
[42] Sarkar S, Banda H, Mitra S. High capacity lithium-ion battery using LiV_3O_8 nanorods. Electrochimica Acta. 2013: **99**: 242–252
[43] Sarkar S, Bhowmik A, Bharadwaj M D, Mitra S. Phase transition, electrochemistry, and structural studies of high Rate $Li_xV_3O_8$ cathode with nanoplate morphology. J. Electrochem. Soc. 2013: **161**: A14-A22.